Proceedings of the Human Factors and Ergonomics Society Annual Meeting
2025, Vol. 69(1) 1068–1073

DOI: 10.1177/10711813251369860
journals.sagepub.com/home/pro
Sage

Applying Engineering Anthropometry to Mitigate Eye Strain in Virtual Environments

Nathan E. Sanders[1] and **Karen B. Chen**[1]

Abstract

This study applies engineering anthropometry and Monte Carlo simulations to define ergonomic guidelines for minimizing vergence-accommodation conflict in virtual environments. Interpupillary distance (IPD) data from three anthropometric datasets (ANSUR I, ANSUR II, CAESAR) were bootstrapped to determine conservative viewing-distance limits accommodating 99% of users. Simulations considered various IPD calibration errors, fixed IPD settings, and focal distances typical of commercial displays. Results established practical zones of comfortable disparity (ZoCD) and vergence to guide virtual interface design.

Keywords

vergence-accommodation conflict, interpupillary distance, Monte Carlo simulation, virtual reality ergonomics, stereoscopic displays, visual fatigue, human-centered design, binocular vision, engineering anthropometry

Introduction

A major ergonomic barrier to using stereoscopic displays is eye strain, and one of the primary causes of eye strain is the vergence-accommodation conflict (Creed et al., 2024; Hirota et al., 2018; Koulieris et al., 2017; Kramida, 2016). These displays present slightly different images to each eye, prompting the eyes to converge (vergence) to maintain single vision, creating the illusion of stereoscopic depth. Meanwhile the eyes remain focused (accommodated) on the display's fixed focal plane. The discrepancy between the convergence angle at this focal plane and the angle required for viewing a virtual object defines the vergence-accommodation disparity or conflict. VR head-mounted displays typically project images through magnifying lenses onto a virtual focal plane located 1–2 m away. For 3D TVs or projectors, the screen itself is the focal plane. Designers can minimize vergence-accommodation conflict by positioning virtual objects close to the focal plane within the Zone of Comfortable Disparity (ZoCD) (Hibbard et al., 2020)

Although the theoretical ZoCD has been extensively studied, for example, regarding optical geometry and subjective visual fatigue (Shibata et al., 2011), as well as the implications of interpupillary distance (IPD) miscalibration (Hibbard et al., 2020), translating these findings into specific ergonomic guidelines remains challenging. A significant barrier is the frequent lack of detailed optical specifications from display manufacturers. Effective ergonomic recommendations also require consideration of IPD calibration policies—whether IPD is individually measured (including measurement errors) or uniformly set across users. Additionally, the equations defining ZoCD limits present analytical difficulties for straightforward percentile-based guidelines, as the resulting distributions are not easily recognizable as any well-known distribution family, despite IPD values themselves being nearly normally distributed (Dodgson, 2004).

Given these challenges, this paper aims to establish practical ergonomic guidelines by applying engineering anthropometry using Monte Carlo simulations. Specifically, the goal is to derive conservative estimates for the near and far limits of the ZoCD, as well as the limit of comfortable vergence, using a design-for-percentiles approach accommodating 99% of users.

Derivations

The ZoCD can be modelled by considering the convergence angle θ at the focal plane distance *s*, which is a function of an

[1]Department of Industrial and Systems Engineering, North Carolina State University, Raleigh, NC, USA

Corresponding Author:
Nathan E. Sanders, Department of Industrial and Systems Engineering, North Carolina State University, 915 Partners Way, Raleigh, NC 27695-7001, USA.
Email: nesander@ncsu.edu

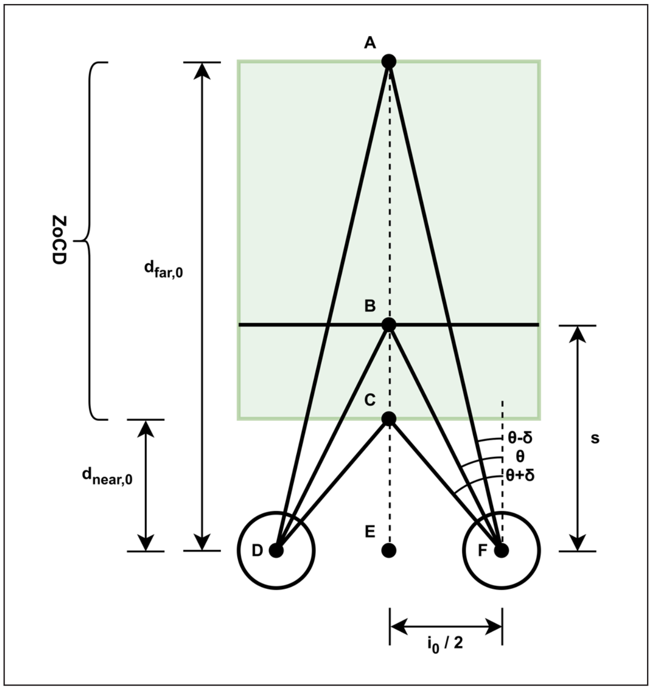

Figure 1. Construction of the ZoCD. The eyes converge to point B on the focal plane *s* with angle θ. The near and far limits of the ZoCD given a tolerable vergence-accommodation disparity δ are points C and A.

individual's IPD i_0. The geometry is shown in Figure 1, which depicts a stylized top view of two eyes converging on the focal plane at point B directly ahead. If the angular disparity that can be comfortably tolerated is δ, then the near and far limits of the ZoCD ($d_{near,0}$ and $d_{far,0}$) correspond to the fixation points C and A at vergence angles $\theta + \delta$ and $\theta - \delta$, respectively.

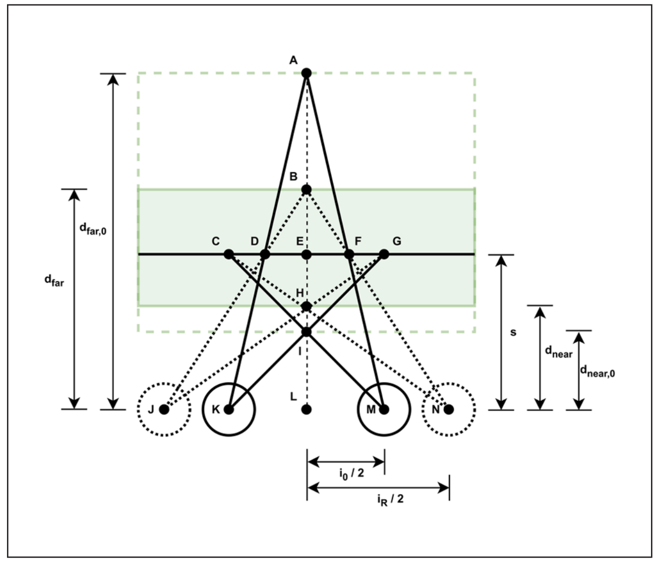

Figure 2. Construction of the ZoCD under miscalibration. Images on the focal plane *s* at points D and F, and C and G intended for rendered (dashed) eyes at J and N cause the eyes to converge on points A and I rather than B and H as intended. The ZoCD is compressed when $i_R > i_0$ (shown) and expands when $i_R < i_0$.

Figure 1 depicts an ideal situation in which the IPD setting on the display (the rendered IPD i_R) is perfectly calibrated to the user's actual IPD i_0. Figure 2 depicts the more realistic situation in which the system's IPD setting is miscalibrated – when the rendered IPD i_R does not equal the user's actual IPD i_0.

In this case the near and far limits of the ZoCD are (with capital letters indicating random variables):

$$D_{near} = \frac{\frac{i_R I_0}{4} s\left(s - \frac{I_0}{2}\tan(\delta)\right)}{\frac{I_0^2}{4}s + \frac{I_0}{2}s^2\tan(\delta) + \frac{(i_R - I_0)I_0}{4}\left(s - \frac{I_0}{2}\tan(\delta)\right)} \tag{1}$$

$$D_{far} = \frac{\frac{i_R I_0}{4} s\left(s + \frac{I_0}{2}\tan(\delta)\right)}{\frac{I_0^2}{4}s - \frac{I_0}{2}s^2\tan(\delta) + \frac{(i_R - I_0)I_0}{4}\left(s + \frac{I_0}{2}\tan(\delta)\right)} \tag{2}$$

A special case occurs when the IPD is over-calibrated ($i_R > i_0$). There will be some finite distance v_{far} at which the eyes are parallel as if they were viewing an object at infinity. Gazing at an object beyond v_{far} will cause the eyes to diverge.

$$V_{far} = s \frac{i_R}{i_R - I_0} \tag{3}$$

Finally, regarding the rendered IPD i_R, consider two IPD-setting policies that might be employed by a user or researcher. In the first, the IPD is set and held constant for all users (Equation 4). This could be the case, for example, if the HMD had only one or a limited number of IPD settings. In the second (Equation 5), the user or researcher attempts to measure and set the IPD but with some measurement error $e \sim N(0, \sigma^2)$.

$$i_R = \{i_1, i_2, i_3\} \tag{4}$$

$$I_R = i_0 + e \tag{5}$$

The challenge of applying a design-for-percentiles approach to Equations 1, 2, and 3, given the IPD setting policies in Equations 4 and 5, lies in modelling their distributions. A non-parametric approach which requires the fewest assumptions is the bootstrap. Although it requires a large dataset of individual IPD measurements (i_0) from which to resample, such datasets are available. Additionally, the distributions of Equations 1, 2, and 3 are conditioned on the assumed distribution of measurement error e, the focal plane distance of the display s, the IPD setting of the device i_R, and the tolerable vergence-accommodation disparity δ. For the results to be translatable, sensible values of these parameters must be selected, and the bootstrap performed on each combination.

Methods

Tolerable vergence-accommodation angular disparity

The comfortable angular disparity δ is about 1–2° (Hibbard et al., 2020). The lower more conservative estimate of 1° was chosen for the simulation.

IPD measurement errors

IPD measurement error was challenging to estimate due to variations in reported statistics such as mean squared error (MSE) and mean absolute error (MAE). A synthesis of available research enabled categorization into three approximate groups: expert, intermediate, and amateur measurements (Han et al., 2023; Holland & Siderov, 1999; McMahon et al., 2012; Murray et al., 2017). Based on these findings, three values of standard deviation were selected for the simulations: 0.5, 1, and 3 mm (Table 1).

Table 1. Estimated Measurement Errors for the Simulation.

Skill level	Method	Error (mm)	σ (mm)
Expert	Pupillometer	0.4–0.6	0.5
	Corneal reflex	0.5–0.8	
	Viktorin's method	0.6–1.0	
Intermediate	Smartphone apps	0.5–1.4	1
	Eye tracker-based	~ 0.4	
	Ruler (trained)	~ 0.6–2.0	
Amateur	Ruler (self, mirror)	~ 3–6	3
	Ruler (friend)	~ 2–4	

Table 2. Summary Statistics for IPD.

Dataset	*n*	Min	Median	Max	Mean	*SD*
ANSUR I	3976	52	63	78	63.4	3.8
ANSUR II	6068	51	63.5	77	63.3	3.7
CAESAR	2382	48.3	66.8	84.6	66.9	5.6

Distribution of IPD

Large samples of individual interpupillary distance measurements (i_0) were obtained from three anthropometric databases: ANSUR I, ANSUR II, and CAESAR. ANSUR I and II are random samples from U.S. military personnel, typically skewed younger than the general population (Dodgson, 2004; Gordon, 1989, 2012). The CAESAR dataset is a convenience sample of adults from the U.S., Europe, and other regions (Robinette et al., 2002), with only the U.S. portion used here. Table 2 summarizes IPD statistics across these datasets.

Focal plane distances of common displays

For projector- or screen-based displays, the focal plane distance is the distance between the user's eyes and the screen, so the reader can measure their own setup. Academic studies using bespoke optical setups have employed focal plane distances ranging from 25 cm to optical infinity (Başak et al., 2019; Korot et al., 2021; Newton, 2022; Pladere et al., 2021, 2022). For commercial headsets, manufacturer specifications are often not published, necessitating a search for unofficial sources. For example, the focal-plane distance of the Quest and Quest 2 was reported as 1.3 m by its lead developer (Carmack, 2021). The HTC Vive's value was estimated as 0.75 m by a Reddit user (u/jensen404, 2016). Microsoft officially publishes the focal-plane distance for the HoloLens 1 and 2 as 2 m (Microsoft Corporation, 2021), whereas Meta has only indirectly suggested an approximate distance of 1 m for the Quest 3 (Meta Platforms, Inc., 2025). Microsoft have also provided guidelines for comfortable viewing distances for the HoloLens 1 and 2 (1.25–5 m), which can later be compared against the simulation results.

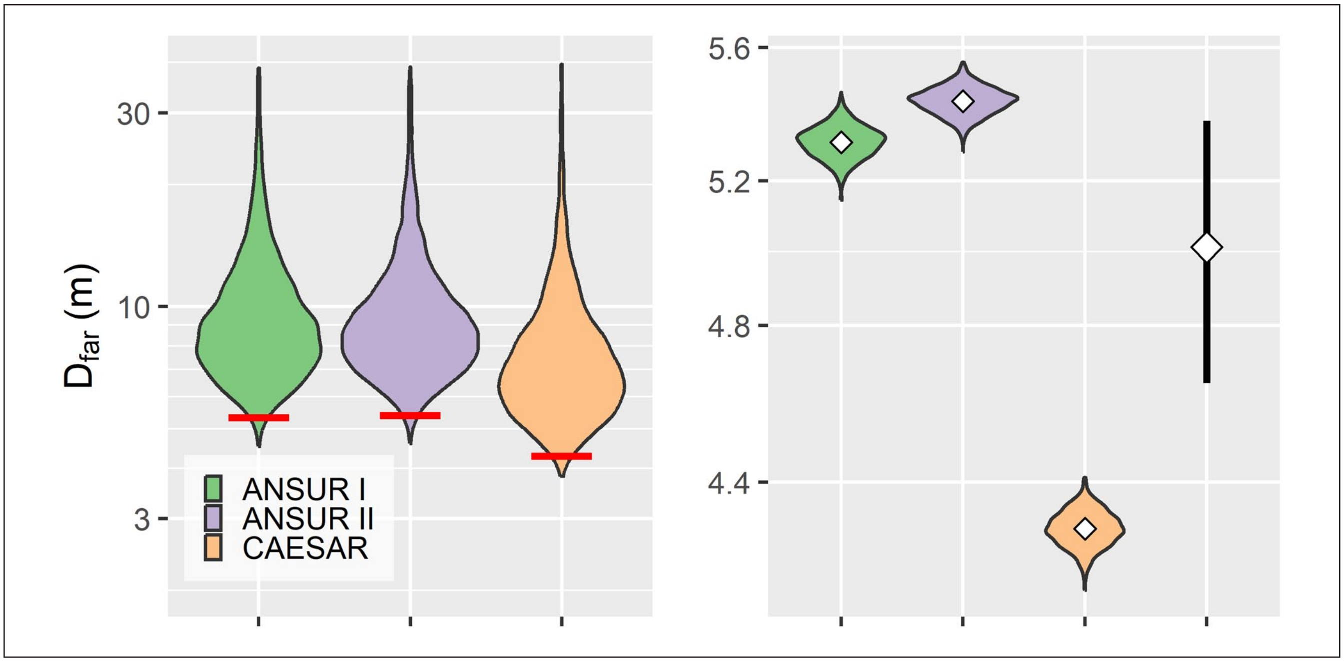

Figure 3. Left: Distribution of a single bootstrap sample of D_{far} for each dataset (s = 1.5 m and σ = 1 mm), with lines marking the 1st percentiles. Right: Distributions of 1st percentiles across bootstrap samples, showing within-group means and between-group mean with ±1 SE (see Figure 4, top-middle).

Fixed IPD settings

Three representative IPD settings for i_R were chosen for simulation—58 mm, 63 mm, and 68 mm—corresponding to the adjustable IPD settings of the Quest 2 headset, and aligning closely with the 10th, 50th, and 90th percentiles of the ANSUR I and II data.

Monte Carlo Procedure

Monte Carlo simulations were performed with each dataset (ANSUR I, ANSUR II, CAESAR) across all combinations of input parameters: three IPD measurement-error levels, three fixed-IPD settings, and a range of focal distances from 1 to 2 meters. Each simulation consisted of 1,000 bootstrap replications, where each replication was a resample (with replacement) matching the size of the original dataset (see Figure 3).

For conditions involving simulated measurement error, random noise was generated from a normal distribution according to Equation 5. From each bootstrap replication, individual near and far limits of the ZoCD and the far limit of comfortable vergence were calculated using Equations 1, 2, and 3. Any negative values in Equations 1 and 2 were set to infinity, reflecting a quirk of the equations.

For each bootstrap replication, the 99th percentile of D_{near} and the 1st percentile of D_{far} and V_{far} were computed. After averaging these percentile estimates across all 1,000 bootstrap replications for each dataset, the results from the three datasets were further averaged. The resulting mean and standard error thus provide estimates of the between-sample variability (Figure 3).

Results

The top row of Figure 4 shows the simulation results for the measured-IPD policy described in Equation 5, where IPD calibration errors are present. The bottom row shows these same statistics for the fixed-IPD policy described in Equation 4, where IPD settings remain constant across users. From left to right, these are the mean 99th percentile of the near limit of comfortable disparity, the mean 1st percentile of the far limit of comfortable disparity, and the mean 1st percentile of the far limit of comfortable vergence.

Discussion

Figure 4 is really a graphical tool to help designers estimate comfortable viewing ranges for any stereoscopic display, and to build virtual environments accordingly. To use it, first select the anticipated IPD calibration policy. If the IPD will be measured and set for every individual, use the top row and select an error estimate (σ) from Table 1. If, on the other hand, the IPD setting will be the same for everyone, use the bottom row and select a setting (i_R) from § *Fixed IPD settings* that most closely matches the setting that will be used. Next, determine the display's focal-plane distance (s) using §

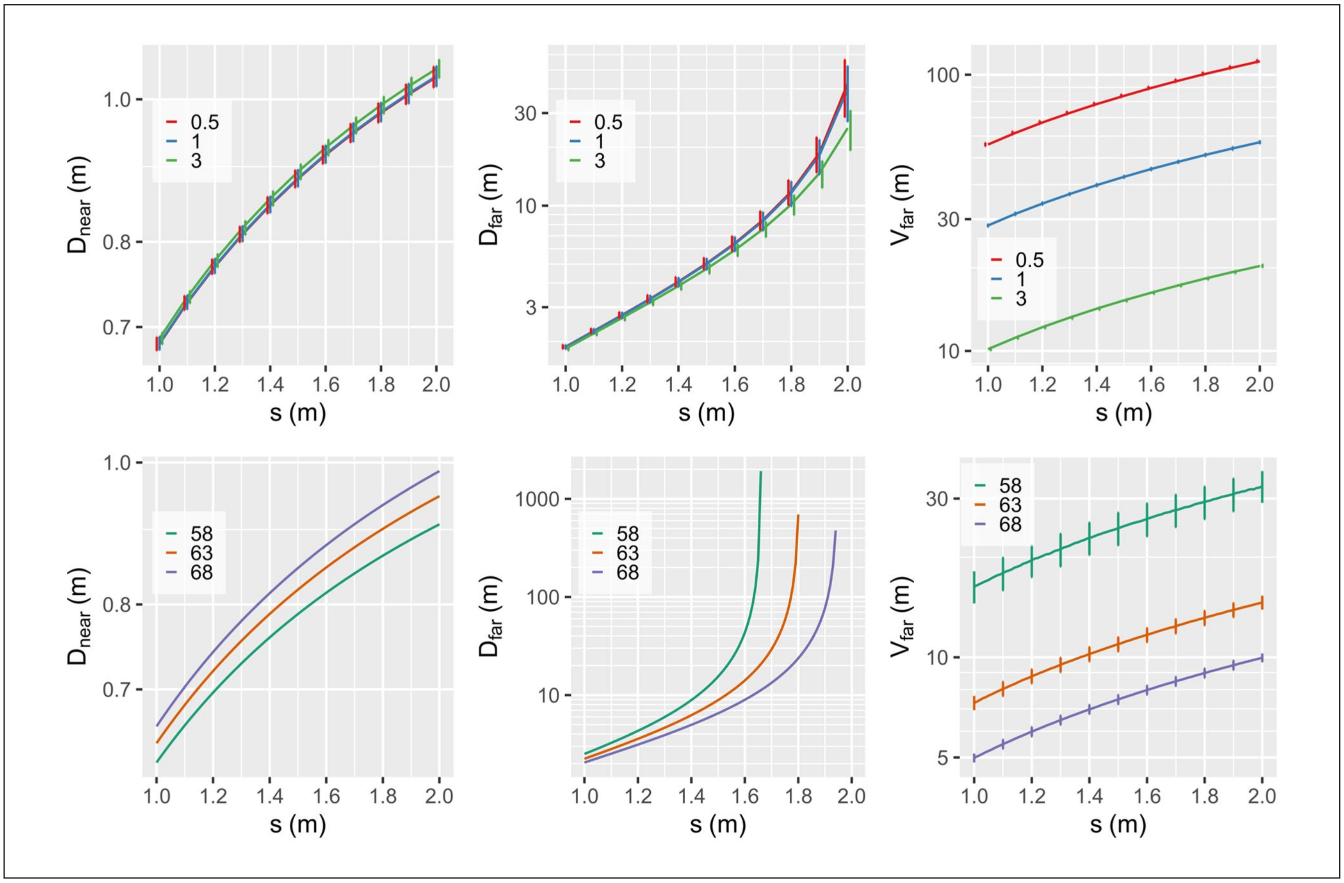

Figure 4. Mean (±1 SE) between-dataset percentile estimates from Monte Carlo simulations. Top row: measured-IPD policy (measurement error σ: 0.5, 1, 3 mm); bottom row: fixed-IPD policy (IPD settings: 58, 63, 68 mm). Columns depict the 99th percentile near limit of ZoCD (left), 1st percentile far limit of ZoCD (middle), and 1st percentile limit of comfortable vergence (right).

Focal plane distances of common displays. Finally, when building the virtual environment, place frequently viewed items like UIs and text between D_{near} (column 1) and the closer of D_{far} (column 2) or V_{far} (column 3).

Consider Alice, a designer preparing an experience for a museum using the HoloLens 2. She does not know what IPD calibration policy the museum will use, but she reasons that a fixed IPD setting at its largest value might be the worst case. In that case, $i_R > i_0$ for most users, so their ZoCD will be compressed (see Figure 2). Referring to § *Fixed IPD settings*, she chooses the largest value of 68 mm. From § *Focal plane distances of common displays*, she selects a focal-plane distance (s) of 2.0 m corresponding to the HoloLens 2. Using the bottom row of Figure 4, she estimates a near limit of comfortable disparity (D_{near}) of about 1 m (bottom-left, purple), a far limit (D_{far}) at infinity (bottom-middle, purple), and a far limit of comfortable vergence (V_{far}) of about 10 m (bottom-right, purple). She therefore designs the AR content so that nearly all elements are rendered within the 1–10 m range, where vergence-accommodation conflict and binocular divergence should (in theory) remain within tolerable limits for about 99% of adults. Microsoft's official comfortable viewing range for the HoloLens 2 is 1.25–5 m, which is more conservative but comparable to the estimate derived here.

Limitations

Because IPD varies significantly with sex, race, and age, the ergonomic guidelines provided will be conservative for user groups with larger average IPDs (e.g., Black, Hispanic, Asian, or Native American men), and optimistic for groups with smaller average IPDs (e.g., White women or adolescents). Second, measurement errors are only rough estimates, so future work might employ a random effects model to estimate measurement errors as more data becomes available. Third, assuming a fixed 1° tolerable vergence-accommodation disparity ignores individual differences and oversimplifies complex physiological realities. Lastly, the simulations assume static viewing conditions along the line of sight, not accounting for off-axis gaze directions.

Acknowledgments

The authors thank Matthew P. Reed at the University of Michigan Transportation Research Institute for graciously providing access to the CAESAR dataset.

Declaration of Conflicting Interests

The authors declared no potential conflicts of interest with respect to the research, authorship, and/or publication of this article.

Funding

The authors disclosed receipt of the following financial support for the research, authorship, and/or publication of this article: This material is based upon work supported by NIOSH (T42 OH008673).

ORCID iDs

Nathan E. Sanders https://orcid.org/0000-0002-0661-0526
Karen B. Chen https://orcid.org/0000-0003-2904-1394

References

Başak, U. Y., Kazempourradi, S., Yilmaz, C., Ulusoy, E., & Urey, H. (2019). Dual focal plane augmented reality interactive display with gaze-tracker. *OSA Continuum*, *2*(5), 1734. https://doi.org/10.1364/OSAC.2.001734

Carmack, J. (2021, March 15). Design focal distance for the Quest/Quest 2 optics. *Twitter (X)*. https://x.com/ID_AA_Carmack/status/1371485209603022853?lang=en

Creed, C., Al-Kalbani, M., Theil, A., Sarcar, S., & Williams, I. (2024). Inclusive AR/VR: Accessibility barriers for immersive technologies. *Universal Access in the Information Society*, *23*(1), 59–73. https://doi.org/10.1007/s10209-023-00969-0

Dodgson, N. A. (2004). Variation and extrema of human interpupillary distance. *Proc. SPIE*, *5291*, 36–46. https://doi.org/10.1117/12.529999

Gordon, C. C. (1989). *1988 Anthropometric Survey of U.S. Personnel: Methods and Summary Statistics* (Technical Report No. NATICK/TR-89/044). U.S. Army Natick Soldier Research, Development and Engineering Center.

Gordon, C. C. (2012). *2012 Anthropometric Survey of U.S. Army Personnel: Methods and Summary Statistics* (Technical Report No. NATICK/TR-15/007). U.S. Army Natick Soldier Research, Development and Engineering Center.

Han K. D., Jaafar M., Stoakes I. M., et al. (2023). Comparing the effectiveness of smartphone applications in the measurement of interpupillary distance. *Cureus*, *15*(7), e42744. https://doi.org/ 10.7759/cureus.42744

Hibbard, P. B., Van Dam, L. C. J., & Scarfe, P. (2020). The implications of interpupillary distance variability for virtual reality. *2020 International Conference on 3D Immersion, IC3D 2020 - Proceedings*, 1–7. https://doi.org/10.1109/IC3D51119.2020.9376369

Hirota, M., Morimoto, T., Kanda, H., Endo, T., Miyoshi, T., Miyagawa, S., Hirohara, Y., Yamaguchi, T., Saika, M., & Fujikado, T. (2018). Objective evaluation of visual fatigue using binocular fusion maintenance. *Translational Vision Science & Technology*, *7*(2), 9. https://doi.org/10.1167/tvst.7.2.9

Holland, B. J., & Siderov, J. (1999). Repeatability of measurements of interpupillary distance. *Ophthalmic and Physiological Optics*, *19*(1), 74–78. https://doi.org/10.1046/j.1475-1313.1999.00400.x

Korot, E., Rolain, M. M., Evans, A., Thanos, A., Bergeles, C., Wood, E. H., & Rolain, M. A. (2021). Purpose-built, head-mounted 3D display for ophthalmic microsurgery: Surgical skill performance and evaluation: A pilot study. *BMJ Innovations*, *7*(2), 463–469. https://doi.org/10.1136/bmjinnov-2020-000507

Koulieris, G.-A., Bui, B., Banks, M. S., & Drettakis, G. (2017). Accommodation and comfort in head-mounted displays. *ACM Transactions on Graphics*, *36*(4), 1–11. https://doi.org/10.1145/3072959.3073622

Kramida, G. (2016). Resolving the vergence-accommodation conflict in head-mounted displays. *IEEE Transactions on Visualization and Computer Graphics*, *22*(7), 1912–1931. https://doi.org/10.1109/TVCG.2015.2473855

McMahon, T. T., Irving, E. L., & Lee, C. (2012). Accuracy and repeatability of self-measurement of interpupillary distance. *Optometry and Vision Science*, *89*(6), 901–907. https://doi.org/10.1097/OPX.0b013e318257f37b

Meta Platforms, Inc. (2025, October 7). *Mixed reality design guidelines. Meta for Developers*. https://web.archive.org/web/20251013230013/https://developers.meta.com/horizon/design/mr-design-guideline

Microsoft Corporation. (2021, October 18). *Comfort. Microsoft Learn*. https://web.archive.org/web/20251013230646/https://learn.microsoft.com/en-us/windows/mixed-reality/design/comfort

Murray, N. P., Hunfalvay, M., & Bolte, T. (2017). The reliability, validity, and normative data of interpupillary distance and pupil diameter using eye-tracking technology. *Translational Vision Science & Technology*, *6*(4), 2. https://doi.org/10.1167/tvst.6.4.2

Newton, D. C. (2022). Human factors considerations for head-worn displays in civil aviation. *Lecture Notes in Computer Science*, *13318*, 233–250. https://doi.org/10.1007/978-3-031-06015-1_17

Pladere, T., Luguzis, A., Zabels, R., Smukulis, R., Barkovska, V., Krauze, L., Konosonoka, V., Svede, A., & Krumina, G. (2021). When virtual and real worlds coexist: Visualization and visual system affect spatial performance in augmented reality. *Journal of Vision*, *21*(8), 17. https://doi.org/10.1167/jov.21.8.17

Pladere, T., Svarverud, E., Krumina, G., Gilson, S. J., & Baraas, R. C. (2022). Inclusivity in stereoscopic XR: Human vision first. *Frontiers in Virtual Reality*, *3*. https://doi.org/10.3389/frvir.2022.1006021

Robinette, K. M., Blackwell, S., Daanen, H., Boehmer, M., & Fleming, S. (2002). *Civilian American and European surface anthropometry resource (caesar), final report. 1. Summary*. US Air Force Research Laboratory.

Shibata, T., Kim, J., Hoffman, D. M., & Banks, M. S. (2011). The zone of comfort: Predicting visual discomfort with stereo displays. *Journal of Vision*, *11*(8), 11–11. https://doi.org/10.1167/11.8.11

u/jensen404. (2016, April 25). *Vive focus distance is ~75 cm* [Online forum post]. *Reddit*. https://web.archive.org/web/20251014004234/https://www.reddit.com/r/Vive/comments/4gbhny/vive_focus_distance_is_75_cm/